

Synthesis and characterisation of polymeric materials consisting of $\{\text{Fe}_2(\text{CO})_5\}$ -unit and their relevance to the diiron sub-unit of [FeFe]-hydrogenase†

Caixia Zhan,^a Xiufeng Wang,^a Zhenhong Wei,^a David J. Evans,^b Xiang Ru,^a Xianghua Zeng^a and Xiaoming Liu^{*a}

Received 20th June 2010, Accepted 14th September 2010

DOI: 10.1039/c0dt00687d

By using “click” chemistry between a diazide and a diiron model complex armed with two alkynyl groups, two polymeric diiron complexes (**Poly-Py** and **Poly-Ph**) were prepared. The two polymeric complexes were investigated using infrared spectroscopy, scanning electron microscopy (SEM), transmission electron microscopy (TEM), thermal gravimetric analysis (TGA), Mössbauer spectroscopy, and cyclic voltammetry (**Poly-Py** only, due to the insolubility of **Poly-Ph**). To probe the coordinating mode of the diiron units in the two polymeric complexes, two control complexes (**3** and **4**) were also synthesised using a monoazide. Complexes **3** and **4** were well characterised and the latter was further crystallographically analysed. It turns out that in both complexes (**3** and **4**) and the two polymeric diiron complexes, one of the two iron atoms in the diiron unit coordinates with one of the triazole N atoms. Our results revealed that both morphologies and properties of **Poly-Py** and **Poly-Ph** are significantly affected by the organic moiety of the diazide. Compared to the protonating behaviour of the complexes **3** and **4**, **Poly-Py** exhibited proton resistance. In electrochemical reduction, potentials for the reduction of the diiron units in **Poly-Py** and hence its catalytic reduction of proton in acetic acid–DMF shifted by over 400 mV compared to those for complexes **3** and **4**. It is likely that the polymeric nature of **Poly-Py** offers the diiron units a “protective” environment in an acidic medium and more positive reduction potential.

1 Introduction

In the course of evolution over a long period, nature “designed” a delicate machinery, [FeFe]-hydrogenase, possessing unique structural and electronic features which render the natural system with a high efficiency and a rapid rate in the catalytic production of dihydrogen and *vice versa*. The key component of this system is the diiron sub-unit as revealed nearly a decade ago,^{1,2} Fig. 1, where the enzymatic catalysis occurs. The view that dihydrogen could

be an alternative green energy vector for our future has greatly stimulated research interest in modelling this diiron sub-unit, which is indicated by the rapid increase in the number of research papers relating to this enzyme. Reviews and publications document well the progress achieved in the past decade in synthesising diiron model complexes which have some of the essential structural features comparable to those found in the enzyme.^{3–14} These achievements not only have greatly advanced our mechanistic understanding of the catalysis of dihydrogen evolution catalysed by systems consisting of low valence iron coordinated by both sulfur and carbon monoxide and other ligands, as well as the enzyme itself, but also the artificial system may bring us a step closer towards assemblies which may be comparable to the natural machinery in the operation of catalysis.

However, to move modelling chemistry further forward, two critical issues need to be tackled, (i) a 3D structured environment is desirable, in which synthetic models are harboured as the diiron sub-unit is within the protein domains in the enzyme and (ii) an appropriate scaffold is needed to combine with synthetic model complexes. With the scaffold, synthetic models could be effectively embedded into matrices in such a way that fabrication of an electrode becomes possible. In such a system the amount of the catalytic components can be delicately tuned and extra functional groups may also be introduced to allow improvements in properties, for example, proton and electron transfer. To this end, there are only a few reports. One approach was immobilisation of a monolayer of diiron model complexes onto the surface of vitreous carbon or gold electrodes.^{15,16} Pickett and co-workers reported the immobilisation of a diiron complex into a polypyrrole film

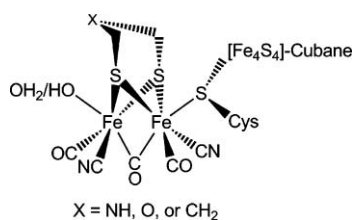


Fig. 1 The diiron sub-unit of the H-cluster of [FeFe]-hydrogenase.^{1,2}

^aDepartment of Chemistry, Institute for Advanced Study, Nanchang University, Nanchang, 330031, China. E-mail: xiaoming.liu@ncu.edu.cn; Fax: +86 (0)791 3969254; Tel: +86 (0)791 3969254

^bDepartment of Biological Chemistry, John Innes Centre, Norwich Research Park, Colney, Norwich, UK NR4 7UH

† Electronic supplementary information (ESI) available: Supplementary figures for related complexes in infrared spectra, schematic structure (complex **3**), cyclic voltammograms, Mössbauer spectra, TEM diagrams, and bond lengths and angles. CCDC reference number 780635. For ESI and crystallographic data in CIF or other electronic format see DOI: 10.1039/c0dt00687d

via diffusion and its subsequent chemical reaction.¹⁷ Resin was also employed by Darensbourg and co-workers as a support to hold model complexes.¹⁸ Most recently, we reported that polyene can be used to integrate diiron units together.¹⁹ To the best of our knowledge, combining polymer materials with a synthetic model had not been reported until this work. In the system described, a polyene-based polymer functionalised with diiron model complexes was achieved via homogeneous polymerisation, the resultant polymer was successfully assembled into an electrode which showed electrochemical activity.

Herein, we develop this approach further. Using “click” chemistry, a well known synthetic strategy,²⁰ between an azide and an alkynyl group under the catalysis of CuI, two polymeric diiron complexes were prepared. The two polymeric materials were characterised using a variety of techniques. One of the polymers (**Poly-Py**) was also electrochemically investigated while the same investigation was not possible for the other one (**Poly-Ph**) due to its poor solubility. The organic moiety bearing the azide groups dictates largely the physical properties and reactivity of the polymeric diiron complexes. This polymeric effect may suggest an approach to achieve novel artificial systems to mimic the diiron sub-unit and its peripheral environment. Such a system may also provide a scaffold for assembling a catalytic electrode.

2. Experimental

2.1 Materials, instrumentation, and general procedures

Reactions and manipulations were performed using standard Schlenk technique under argon when air-/moisture-sensitive materials were handled. In extreme cases, handling was carried out in an inert atmosphere box (Braun Lab-star). All solvents were dried following standard methods, distilled prior to use and stored under an argon atmosphere. General chemicals were purchased from local commercial suppliers and further purifications were performed when necessary. More specific chemicals were purchased from Sigma-Aldrich and Alfa-Aesar. Diiron hexacarbonyl complex, $[\text{Fe}_2(\mu\text{-SCH}_2\text{CCH})_2(\text{CO})_6]$, and 11-azidoundecan-1-ol were prepared as described in our recent work.¹⁹

Infrared spectra were recorded on Scimitar 2000 (Varian). NMR spectra were recorded on Avance DRX 400 (Bruker) and Avance 600 (Bruker) in CDCl_3 . Scanning electron microscope (SEM) images were obtained on Quanta 200F. Transmission electron microscope (TEM) images were obtained on JEM2100. Thermal gravimetric analysis (TGA) measurement was carried out on TA SDT Q600 at a heating rate of 20 K min^{-1} under a nitrogen purge. Mössbauer spectra were recorded in zero magnetic field at 80 K on an ES-Technology MS-105 Mössbauer spectrometer with a 220 MBq ^{57}Co source in a rhodium matrix at ambient temperature. Spectra were referenced against a 25 μm iron foil at 298 K and spectral parameters were obtained by fitting with Lorentzian curves. The X-ray single crystal diffraction data were collected on Bruker Smart CCD diffractometer with graphite-monochromated $\text{Mo-K}\alpha$ radiation ($\lambda = 0.71073 \text{ \AA}$).

Electrochemical investigations were performed under argon in a customised glass cell with a three-electrode system as described elsewhere.²¹ In the setup, the working electrode was a glassy carbon disc ($\phi = 1 \text{ mm}$) and a glassy carbon strip electrode was used as a counter electrode. Ag/AgCl was used as reference electrode whose

inner reference solution is composed of $0.05 \text{ mol L}^{-1} [\text{NBu}_4]\text{Cl}$ and $0.45 \text{ mol L}^{-1} [\text{NBu}_4]\text{BF}_4$. In 0.5 mol L^{-1} dichloromethane, the potential of the ferrocenium/ferrocene couple is 0.55 V against this reference electrode. All potentials were quoted against the ferrocenium/ferrocene couple.

A typical procedure for electrochemistry is as follows. Under an Ar atmosphere, **Poly-Py** (20.2 mg) was added into $0.1 \text{ mol L}^{-1} [\text{NBu}_4]\text{BF}_4\text{-DMF}$ solution (4.0 mL). A scan rate of 0.1 V s^{-1} was used unless otherwise stated. In the investigation of catalytic reduction, acetic acid was successively added in an appropriate amount into the electrochemical cell and cyclic voltammetry was accordingly measured.

2.2 Synthesis of the diazides, 2 and 2'

2.2.1 Preparation of the dibromides, 1 and 1'. A mixture of AIBN (azobisisobutyronitrile, 100.4 mg, 0.61 mmol) and NBS (*N*-bromosuccinimide, 10.70 g, 60.12 mmol) were dissolved in CCl_4 (100 mL), to which 2,6-dimethylpyridine (3.5 mL, 30 mmol) was then added. The mixture was vigorously stirred to achieve a light yellow mixture and then irradiated with 200 W tungsten-bulb light under reflux for 12 h, the light yellow mixture turned finally brown. After being cooled to room temperature, the reaction mixture was filtered to remove any insoluble solids. Removal of the solvent produced an oily residue which was purified using flash chromatography on silica gel (ethyl acetate/petroleum ether = 1: 6) to give a white crystalline solid (1.28 g, 17%), 2,6-dibromomethylpyridine (**1**). M.p. $92 \text{ }^\circ\text{C}$ (uncorrected), $^1\text{H NMR}$ (CDCl_3 , 295.5 K): 4.548 (s, CH_2 , 4H), 7.377 (d, *Py*, 2H, $J = 7.76 \text{ Hz}$), 7.720 (q, *Py*, 1H).

The other dibromide, 1,3-dibromobenzene (**1'**), was analogously prepared as a white crystalline solid (4.56 g, 29%). Mp $78 \text{ }^\circ\text{C}$ (uncorrected). $^1\text{H NMR}$ (CDCl_3 , 295.5 K): 4.49 (s, CH_2 , 4H), 7.33 (m, *Ph*, 3H), 7.42 (s, *Ph*, 1H).

2.2.2 Preparation of the diazides, 2 and 2'. To a suspension of NaN_3 (6.50 g, 100.0 mmol) in DMF (50 mL) was added 2,6-bis(bromomethyl)pyridine (1.75 g, 6.67 mmol). The mixture was heated whilst stirring at $70 \text{ }^\circ\text{C}$ for 10 h. Water (100 mL) was added to the reaction when being cooled to room temperature. Extraction with ether ($3 \times 50 \text{ mL}$) was performed and all the extracts were combined and washed with brine ($3 \times 20 \text{ mL}$). After being dried with MgSO_4 , the solvent was evaporated under reduced pressure to give a liquid residue. The residue was purified using flash chromatography on silica gel (ethyl acetate/petroleum ether = 1: 3) to produce a colourless oil (1.22 g, 96%). IR (KBr): ($-\text{N}_3$) 2104 cm^{-1} . $^1\text{H NMR}$ (CDCl_3 , 295.5 K): 4.477 (s, CH_2 , 4H), 7.296 (d, *Py*, 2H, $J = 7.60 \text{ Hz}$), 7.764 (q, *Py*, 1H).

1,3-bis(azidomethyl)benzene, **2'**, a colourless liquid (0.91 g, 84%) was prepared similar to compound **2**. IR (KBr): ($-\text{N}_3$) 2099 cm^{-1} . $^1\text{H NMR}$ (CDCl_3 , 295.5 K): 4.38(s, $-\text{CH}_2$, 4H), 7.30(m, *Ph*, 3H), 7.41(t, *Ph*, 1H).

2.3 Cyclisation between the diiron hexacarbonyl complex, $[\text{Fe}_2(\mu\text{-SCH}_2\text{CCH})_2(\text{CO})_6]$, and the diazide compounds via “click” chemistry

A red solution of $[\text{Fe}_2(\mu\text{-SCH}_2\text{C}\equiv\text{CH})_2(\text{CO})_6]$ (1.20 g, 2.84 mmol) in THF (40 mL) was added to a solution of Et_3N (2.40 mL) and CuI (17.07 mg, 0.09 mmol) in THF (10 mL) followed by

the addition of diazide **2** (0.54 g, 2.84 mmol). After stirring overnight at 40 °C the reaction solution turned from red to a black suspension. The suspension was poured into ethyl acetate (1000 mL) with vigorous stirring for 10 min, after standing for 48 h, a black precipitate formed on the bottom of the reaction vessel. The solid was collected by filtration, washed successively with THF (250 mL), H₂O (100 mL), Et₂O/EtOH 1 : 1 (250 mL) and finally Et₂O (250 mL). The obtained black solid, **Poly-Py** (0.66 g), was dried in vacuum.

Reaction of diazide **2'** (0.37 g, 1.99 mmol) with the same diiron hexacarbonyl complex (0.84 g, 1.96 mmol) produced a pale brown solid, **Poly-Ph** (0.54 g). The preparation was identical to that for **Poly-Py** except that methanol rather than ethyl acetate was used as precipitating solvent.

2.4 Synthesis of Fe₂(μ-SCH₂C≡CH)(μ-SCH₂R)(CO)₆ (R = (CH₂)₁₁OH, **3**; R = CH₂Ph, **4**)

A red solution of [Fe₂(μ-SCH₂C≡CH)₂(CO)₆] (0.26 g, 0.61 mmol) in THF (20 mL) was added to a solution of Et₃N (0.38 g, 0.5 mL) and CuI (7.3 mg, 0.04 mmol) in THF (10 mL). To the mixture was added 11-azidoundecan-1-ol (0.13 g, 0.61 mmol). After stirring at 40 °C for 3.5 h the red reaction solution turned to a brown suspension. The solvent was evaporated under reduced pressure and the product was purified using flash chromatography on silica gel (ethyl acetate/petroleum ether = 1 : 2) to give a dark red solid **3** (0.12 g, 48%). Layering its solution in dichloromethane with hexanes produced dark-red plate-shaped crystals. IR (DCM): (CO) 2041, 1996, 1966, 1937 cm⁻¹, (-C≡CH): 3305 cm⁻¹. ¹H NMR (CDCl₃, 295.5 K): 1.5–1.19 (m, H_c, 18H), 1.83 (H_a, 1H), 2.26 (s, H_h, 1H), 2.47–2.34 (m, H_g, 2H), 3.66–3.30 (m, H_{f+b}, 4H), 4.23 (tri, H_d, 2H), 7.24 (s, H_e, 1H) (please refer to Fig. S3† for the labeling scheme of its non-CO carbon atoms). Microanalysis of complex **3** (C₂₂H₂₉Fe₂N₃O₆S₂, MW = 607.30), calc. (found): C%, 43.51 (44.25); H%, 4.81 (4.43); N%, 6.92 (7.20).

By analogy, reacting azidomethylbenzene (0.16 g, 1.2 mmol) with [Fe₂(μ-SCH₂C≡CH)₂(CO)₆] (0.51 g, 1.2 mmol) produced a dark red solid (complex **4**) (0.12 g, 19%). Its solution in DCM layered with hexanes produced crystal blocks suitable for X-ray single crystal diffraction analysis. IR (DCM): (CO) 2041, 1997, 1967, 1942 cm⁻¹, (-C≡CH): 3303 cm⁻¹. ¹H NMR (CDCl₃, 295.5 K): 2.26 (s, -C≡CH, 1H), 2.47–2.34 (m, CH₂, 2H), 3.61–3.26 (m, CH₂, 2H), 5.42 (d, CH₂, 2H, J = 11.7 Hz), 7.39–7.11 (m, Ph, 5H), 7.53 (s, triazol, 1H). Microanalysis for complex **4** (C₁₈H₁₃Fe₂N₃O₅S₂, MW = 527.13), calc. (found): C%, 41.01 (40.12); H%, 2.49 (3.12); N%, 7.97 (7.68). Please note that the relatively large discrepancy between the calculated and the determined values may result from involvement of moisture during the operation: **4**·0.5H₂O, calc. (found): C%, 40.32 (40.12); H%, 2.63 (3.12); N%, 7.84 (7.68).

2.5 Crystal structure determination

The crystal structure of complex **4** was solved using direct methods and refined on F² using full-matrix least-squares methods with the *SHELXL-97* program.²² All non-H atoms were anisotropically refined. All H atoms were geometrically placed in idealised positions (C–H = 0.99 Å, with U_{iso}(H) = 1.2U_{eq}(C) for methylene groups; C–H = 0.95 Å, with U_{iso}(H) = 1.2U_{eq}(C) for aromatic

ring; C–H = 0.93 Å, with U_{iso}(H) = 1.2U_{eq} for alkyne group) and constrained to ride on their parent atoms.

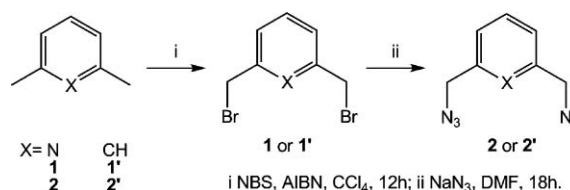
2.6 Reaction of Poly-Py with acid HBF₄

Poly-Py (10.0 mg) was dissolved in DMF (6 mL). To the solution was added acid HBF₄ (6.4 μL) under CO. Infrared spectra were recorded before and after the addition of the acid. The behaviour of complex **3** upon the addition of the acid was examined in the same manner.

3 Results and discussion

3.1 Synthesis

The synthesis of diazides is shown in Scheme 1. Bromination of 2,6-bis(azidomethyl)pyridine and 1,3-bis(azidomethyl)benzene, respectively, produced the dibromides (**1** and **1'**), which were further reacted with sodium azide in dimethylformide (DMF) to give the desired diazides in yields over 90%.



Scheme 1 Synthesis of the diazides.

3.2 Formation of the two polymeric complexes, Poly-Py and Poly-Ph

The “click” reaction of the diiron carbonyl complex, [Fe₂(μ-SCH₂C≡CH)₂(CO)₆], and diazides **2** and **2'** under the catalysis of CuI in THF generated polymeric diiron complexes, **Poly-Py** and **Poly-Ph**, respectively, Scheme 2. Successful cyclisation between the azides and the diiron complex was confirmed by the characteristic absorptions of triazole rings ranging from 1400 to 1600 cm⁻¹, Fig. 2. The strong absorption bands between 2100 and 1850 cm⁻¹ suggest the existence of carbonyl groups in the prepared polymeric

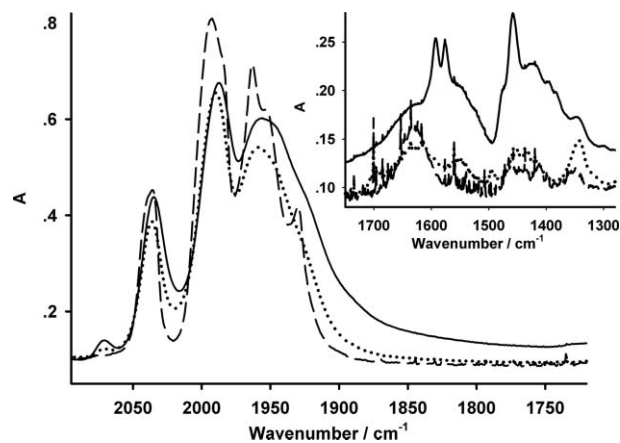
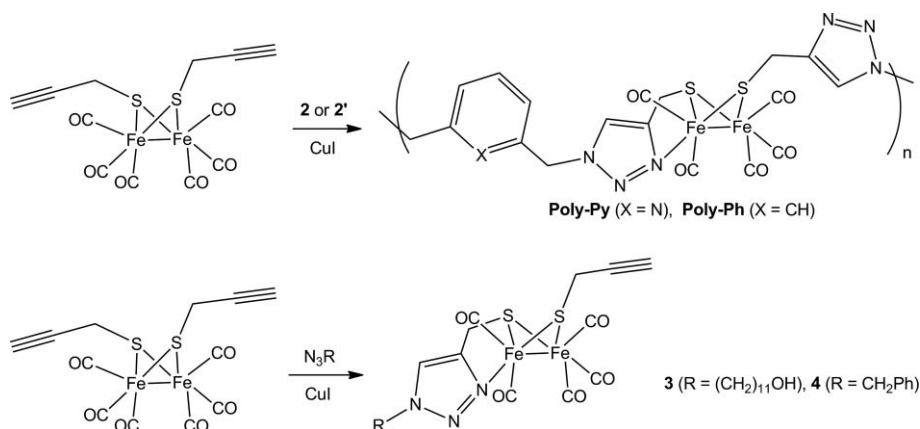


Fig. 2 IR spectra (carbonyl region) of **Poly-Py** (solid line), **Poly-Ph** (dot line) and complex **3** (dash line) (KBr). Inset: spectral region for the triazol ring.



Scheme 2 Synthesis of **Poly-Py**, **Poly-Ph**, and complexes **3** and **4** via “click” chemistry.

materials. It is noteworthy that the rather weak absorption band at around 2070 cm⁻¹ in the infrared spectra of the two polymeric complexes is likely attributed to terminal diiron hexacarbonyl units of the polymeric chains. The broadness of those absorption bands indicates the polymeric nature of the two materials.

Further examination of their spectral patterns reveals a high similarity to those of diiron pentacarbonyl complexes reported in the literature.^{23–27} As shown in Fig. 2, both materials possess an identical spectral pattern, which rules out the possibility that the pyridinyl N atom is involved in the formation of the diiron pentacarbonyl unit in **Poly-Py** since both polymeric materials exhibit nearly superimposable spectral profiles. In other words, one of the triazolyl N atoms may coordinate to one of the Fe(1) atoms in the diiron unit. To confirm this proposed coordinating mode, two monomeric diiron complexes **3** and **4** were prepared from the reaction of [Fe₂(μ-SCH₂C≡CH)₂(CO)₆] with 11-azidoundecan-1-ol and benzylazide, respectively, Scheme 2.

The identities of complexes **3** and **4** were well established using infrared spectroscopy, NMR, and micro analysis. As shown in Fig. 2 and Fig. S4† (infrared spectrum of complex **4**), their spectral profiles are highly similar to those of the two polymeric complexes. Complex **4** was further crystallographically analysed. As shown in Fig. 3, this complex shows largely the structural features found for analogous diiron pentacarbonyl complexes reported in the literature.^{4,9,14,24,26,28,29} But it is noteworthy that the Fe–N bond is *trans* rather than *cis* to one of the two sulfur atoms as found in those reported analogues. The triazole ring is co-planar with the one defined by Fe2, S2, C9, C10, and N1 atoms. Crystallographic details for this complex are tabulated in Table 1.

The diiron centres in both polymeric materials were examined using Mössbauer spectroscopy, Fig. S6.† Both **Poly-Py** and **Poly-Ph** show slightly asymmetric, broad doublets, particularly **Poly-Ph**. The measured parameters (mm s⁻¹) are isomer shift (i.s.) = 0.15, quadrupole splitting (q.s.) = 1.01 (**Poly-Py**) and i.s. = 0.42, q.s. = 0.84 (**Poly-Ph**), respectively. Except for the parameters for **Poly-Ph**, the values are comparable to those for both diiron pentacarbonyl and diiron hexacarbonyl complexes with an {Fe^IFe^I} core.^{19,25} However, it must be noted that the spectrum for a diiron pentacarbonyl complex can be more complicated than that for a diiron hexacarbonyl complex.²⁵ On the other hand, higher oxidation state irons may exist as impurities in the material, which gives a high value of i.s. as observed in our recent work.¹⁹

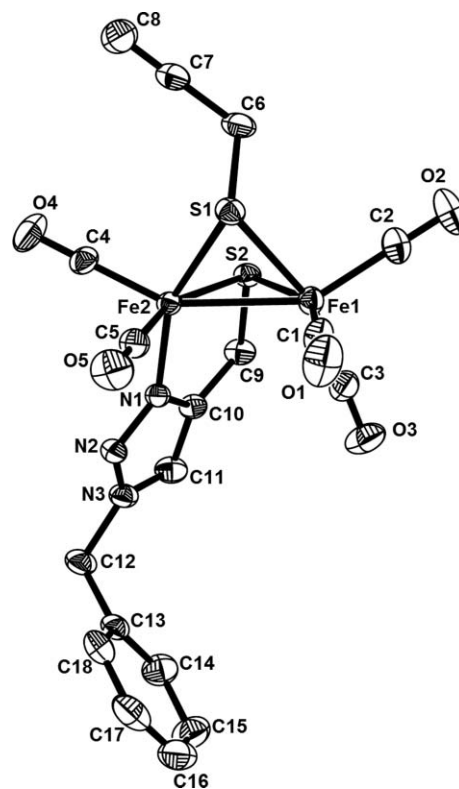


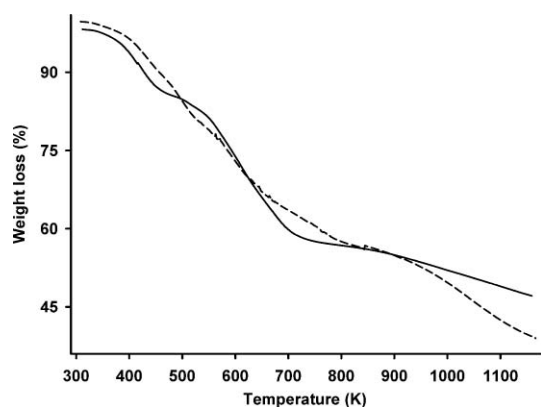
Fig. 3 Crystal structure of complex **4** (the ellipsoids were drawn at a thermal probability of 30% and all hydrogen atoms are omitted for clarity) and selected bond lengths (Å) and bond angles (°): Fe(1)–Fe(2) = 2.5411(4); Fe(2)–N(1) = 1.9655(13); Fe(1)–S(1) = 2.2630(5); Fe(1)–S(2) = 2.2893(5); Fe(2)–S(1) = 2.2236(5); Fe(2)–S(2) = 2.2447(5); ∠Fe(2)–S(1)–Fe(1) = 68.988(15); ∠Fe(2)–S(2)–Fe(1) = 68.166(14); ∠N(1)–Fe(2)–S(1) = 157.17(4); ∠N(1)–Fe(2)–Fe(1) = 101.01(4).

It is difficult, therefore, to precisely analyse the Mössbauer data.

Thermal gravimetric analysis (TGA) of the two polymeric complexes shows that three main stages of decomposition were observed, roughly from 300 K to 470 K, 540 K to 720 K, and 720 K to 1100 K, Fig. 4. This behaviour is, more or less, like that for the polyene material functionalised with {Fe₂(CO)₆} units we reported recently.¹⁹ It was found that the first stage of the decomposition

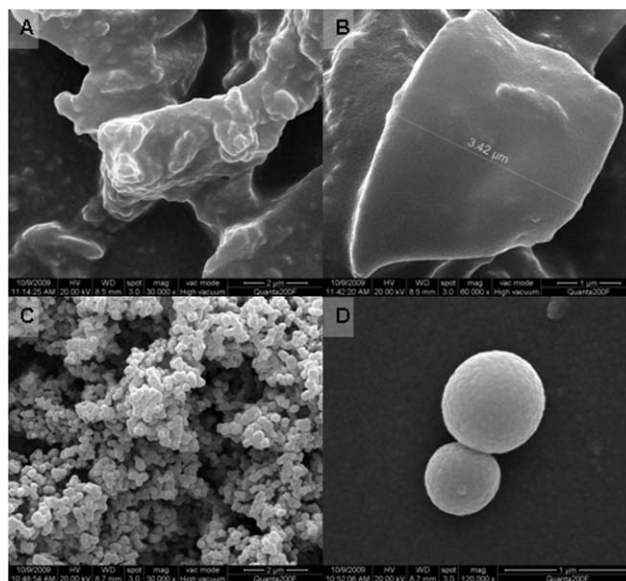
Table 1 Crystal data and structure refinement for complex **4** (CCDC 780635)

Empirical formula	$C_{18}H_{13}Fe_2N_3O_5S_2$
Formula weight	527.15
Temperature	296(2) K
Wavelength	0.71073 Å
Crystal system, space group	Triclinic, $P\bar{1}$
Unit cell dimensions	$a = 7.8501(9)$ Å, $\alpha = 81.0330(10)^\circ$ $b = 8.1409(9)$ Å, $\beta = 84.0780(10)^\circ$ $c = 18.077(2)$ Å, $\gamma = 71.5380(10)^\circ$
Volume	$1080.6(2)$ Å ³
Z, Calculated density	2, 1.620 Mg m ⁻³
Absorption coefficient	1.570 mm ⁻¹
$F(000)$	532.0
Crystal size	$0.49 \times 0.45 \times 0.12$ mm
Theta range for data collection	2.66 to 28.43°
Limiting indices	$-10 \leq h \leq 10$, $-10 \leq k \leq 10$, $-24 \leq l \leq 24$
Reflections collected/unique	10273/5442 [$R(\text{int}) = 0.0168$]
Completeness to theta = 28.43	96.8%
Absorption correction	Semi-empirical from equivalents
Refinement method	Full-matrix least-squares on F^2
Data/restraints/parameters	5442/0/271
Goodness-of-fit on F^2	1.003
Final R indices [$I > 2\sigma(I)$]	$R_1 = 0.0264$, $wR_2 = 0.0705$
R indices (all data)	$R_1 = 0.0332$, $wR_2 = 0.0752$
Largest diff. peak and hole	0.460 and -0.186 e Å ⁻³

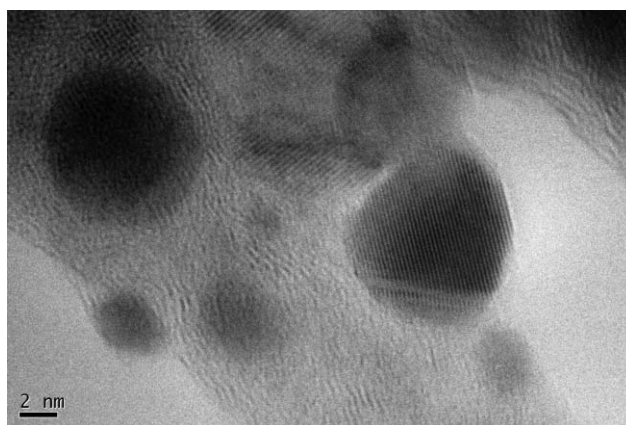
**Fig. 4** TGA diagrams of **Poly-Py** (dash line) and **Poly-Ph** (solid line) measured under nitrogen flow at a heating rate of 20 K min⁻¹.

is due to CO-loss. By analogy, the first stage decomposition shown in Fig. 4 is attributed to the decomposition of the diiron-carbonyl units. The major difference comes from the decomposition pattern after losing CO. The polyene showed a simpler pattern for its thermal decomposition. This difference originates from the difference in the composition of these polymers. In the previously reported polyene, its diiron units dangle at its backbone whereas in both **Poly-Py** and **Poly-Ph**, the diiron unit is one of the building blocks to constitute the polymeric backbone along with the moiety of the diazide. Thus, at the stage of losing CO, it is expected that the polymeric chain breaks into smaller fragments. On further heating these fragments undergo more complicated thermal decomposition compared to the polyene-based material.

The morphology of the two polymeric complexes, **Poly-Py** and **Poy-Ph**, were explored using both scanning and transmission electron microscopies. Fig. 5 shows SEM images of the two polymeric complexes, which reveal rather different morphologies. **Poly-Py** is essentially plate-like whereas **Poy-Ph** has a spherical shape with a diameter of approximately 500 nm. This difference

**Fig. 5** SEM diagrams of the two polymeric complexes: **Poly-Py** (A and B) and **Poly-Ph** (C and D).

in morphology is undoubtedly ascribed to the nature of the organic moiety which bears the two azide groups since the only difference between **Poly-Py** and **Poy-Ph** is the aromatic ring (Scheme 2). The variation in the organic skeleton not only changes drastically their morphology, but also their solubility. **Poly-Py** is highly soluble in DMF and DMSO, and slightly soluble in polar solvents such as ethanol. But **Poly-Ph** is hardly soluble in any common organic solvents. TEM images also indicate a significant difference in internal structure between **Poly-Py** and **Poly-Ph** (Fig. 6 and S7†). For the former, regular linear arrays and even possibly orthogonal stacking structures were observed, Fig. 6. These structural features were hardly found for **Poly-Ph** (Fig. S7†). The controlling role played by the organic part in the diazide in governing the properties of the polymeric complexes suggests that varying the organic moiety would be an effective approach to tune materials of this type to achieve desired properties, for example, hydrophilicity and basicity. This work is currently underway in our laboratory. Although estimation of its molecular weight turned out

**Fig. 6** TEM diagram of **Poly-Py** showing both the linear arrays and possibly orthogonal stacking structures.

unsuccessful using a static light scattering technique, the length of the linear arrays (up to 300 Å, Fig. S8†) may give a clue about the number of diiron units in the linear chain of the polymer. By considering the curling effect of the polymer chain, it is sensible to assume that each unit takes up about 10 Å or less. Therefore, the number of the diiron unit estimated could be over 30. Despite the linear arrays observed in the TEM image of **Poly-Py**, the internal structure (3D-structure) of both polymers is unknown.

3.3 Reaction of **Poly-Py** with the acid, HBF_4

As discussed earlier, the diiron units in the two polymeric complexes exist in the form of diiron pentacarbonyl. For diiron model complexes of this coordinating mode, it has been well established that bridging hydrides formed upon protonation and under CO atmosphere, these hydrides could be converted to diiron hexacarbonyl complexes.^{24,26} But addition of HBF_4 acid into a solution of the polymer in DMF did not produce either bridging hydrides or protonated species. The acid has hardly any effect on the diiron units, Fig. S1.†

To have a better understanding of the action upon the addition of the acid, complex **3** which possesses the essential structural feature of the diiron units in **Poly-Py** was reacted with the acid in the same manner. Results showed that protonation is observed but not as clean as those analogues reported previously.^{24,26} Although some absorption bands around 2100 cm^{-1} may be an indication of forming either a bridging hydride or perhaps a diiron hexacarbonyl species, most of the complex decomposed upon the addition of the acid, which is in strong contrast to the inertness of **Poly-Py** upon addition of the acid. Neutralisation of the mixture after the acid addition did recover a very small portion of the parent complex **3**, Fig. S2.† This further supports its partial protonation as described above.

The sharply contrasting behaviours in the reaction with the acid indicate that in the polymeric form, the diiron units can not be protonated, which ought to be attributed to its polymeric nature. This may be a rationalisation of our initial idea that a polymeric system into which a model complex is incorporated may offer the metal centre a “protective” environment *via* the 3D structure of the polymer system. Although it was not intended that the polymeric complex **Poly-Py** was stable in the acidic medium, our results, indeed, open up the possibility of a novel approach in modelling the diiron sub-unit and the peripheral environment of the $[\text{FeFe}]$ -hydrogenase.

3.4 Electrochemical investigations

We are particularly interested in the electrochemical behaviour of the synthesised polymeric materials due to their relevance to electrocatalytic reduction of protons. Although the electrochemical investigation of **Poly-Py** was entirely hampered since it is insoluble in any solvent, a reasonable solubility of **Poly-Py** in DMF allowed such an investigation. For comparison, both of the control complexes **3** and **4** were also electrochemically examined. As shown in Fig. 7 and Fig. S5,† complexes **3** and **4** exhibit nearly identical electrochemical reductions to diiron pentacarbonyl analogues reported in the literature^{23,25,27} except that the reduction occurs at a slightly more negative potential, which is probably ascribed to the decent electron-donating ability of the coordinated

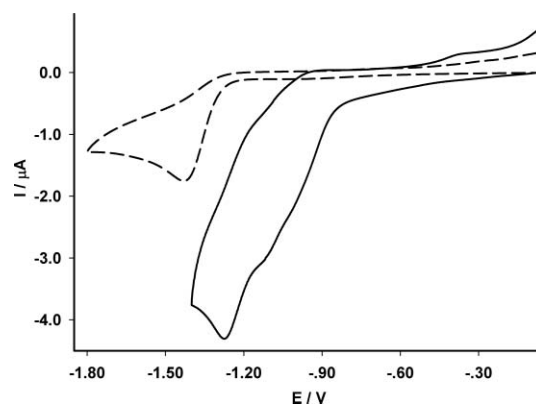


Fig. 7 Cyclic voltammograms of **Poly-Py** (5.1 mg mL⁻¹, solid line) and complex **3** (5.7 mmol L⁻¹, dash line) in 0.1 mol L⁻¹/DMF solution at a scan rate of 0.1 V s⁻¹ (298 K).

triazole ring. The electrochemical reduction of **Poly-Py** is shown in Fig. 7, which exhibits a sharp difference to that of complex **3** in both reduction potential and electrochemical profile. The broadness of the reduction process originates probably from the polymeric nature of **Poly-Py** in which a range of macromolecules possessing different numbers of diiron units exist. The striking feature of the reduction of **Poly-Py** is the significant positive shift in potential (*ca.* 400 mV based on the potential where the reduction begins). As suggested by its infrared spectral absorption bands and Mössbauer parameters, the diiron pentacarbonyl unit essentially retains its structure in the polymeric material similar to that of complex **4** (Fig. 3). Therefore, it is sensible that this significant shift in reduction potential is correlated to the well known electron-withdrawing nature of the diiron unit in the same macromolecule.

Despite the inertness of **Poly-Py** against protonation (*vide ante*), this polymeric material shows catalytic reduction of protons in a medium of acetic acid/DMF upon reduction, Fig. 8. It has been well reported that the reduction of diiron complexes of the core, $\{\text{Fe}_2(\text{CO})_X\}$ ($X = 4-6$) is complicated due to their reduction processes coupling to chemical reactions.^{3,6,8,12,27,30-38} In catalysis of proton reduction, the catalytic species is not simply the monoanion

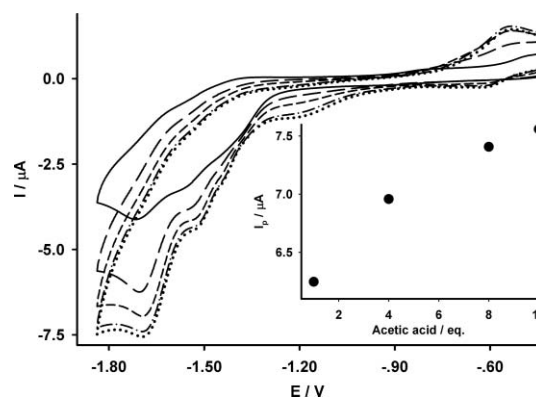


Fig. 8 Cyclic voltammograms of **Poly-Py** (5.1 mg mL⁻¹) in 0.1 mol L⁻¹/DMF solution in the presence of acetic acid (0.0, 1.0, 4.0, 8.0, 10.0 eq.) at a scan rate of 0.1 V s⁻¹ (298 K). Inset: Plot of the catalytic peak current against the concentration of the acid.

$\{\text{Fe}_2(\text{CO})_x\}^{-1}$, instead its protonated form, for example, hydride after being further reduced at a more positive potential compared to that of the initial reduction is probably responsible for the catalysis.^{30,33,35,39} This mechanistic complication may explain the positive shift in the peak potential observed for complex **3** on variation of the acid concentration, Fig. 9. Such a positive shift was also observed in the catalysis of proton reduction with the presence of **Poly-Py** as shown in Fig. 8, which suggests that this polymeric complex may adopt a similar catalytic mechanism.

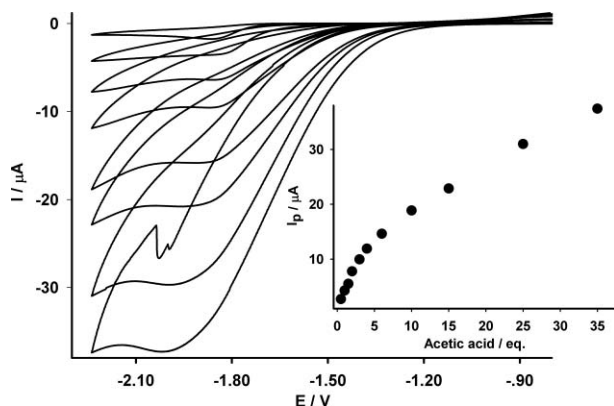


Fig. 9 Cyclic voltammograms of complex **3** (5.7 mmol L^{-1}) in 0.1 mol L^{-1} DMF in the presence of acetic acid (0.0, 1.0, 2.0, 4.0, 10.0, 15.0, 25.0, 35.0 eq.) at a scan rate of 0.1 V s^{-1} (298 K). Inset: Plot of the catalytic peak current against the concentration of the acid.

4 Conclusions

Two polymeric diiron complexes as mimicking systems for the [FeFe]-hydrogenase were prepared using “click” chemistry. Except for the terminal diiron unit, the other diiron unit exists as a pentacarbonyl core, $\{\text{Fe}_2(\text{CO})_5\}$, in which one of the iron atoms coordinates to the N1 atom of the triazole ring. Such a coordinating mode was confirmed employing two control complexes (**3** and **4**). The infrared spectra of the two complexes show a great similarity to the polymeric complexes and further, complex **4** was crystallographically analysed. Due to the polymeric effect, **Poly-Py** shows stability against the acid HBF_4 as well as a positive shift in reduction potential (*ca.* 400 mV) in DMF compared to complexes **3** and **4**. Our results suggest that the diiron sub-unit of the enzyme could be modelled in such a way that the dimetallic centre is harboured in a “protective” environment, offered by the polymeric system, and that the surrounding polymer through finely tuning the organic moiety can possess the desired physical and chemical properties, for example, hydrophilicity and basicity. Incorporating the diiron units into polymeric systems may also provide a platform to assemble a catalytic electrode, which is one of the major goals of modelling the enzyme.¹⁹

Acknowledgements

We thank NSF (China) (Grant No: 20871064), Ministry of Science and Technology (China) (973 program, Grant No: 2009CB220009), and the State Key Laboratory of Coordination Chemistry at Nanjing University (China) for financial support.

The BBSRC (UK) supports DJE through a Core Strategic Grant to the John Innes Centre.

References

- 1 J. W. Peters, W. N. Lanzilotta, B. J. Lemon and L. C. Seefeldt, *Science*, 1998, **282**, 1853–1858.
- 2 Y. Nicolet, C. Piras, P. Legrand, C. E. Hatchikian and J. C. Fontecilla-Camps, *Structure*, 1999, **7**, 13–23.
- 3 C. Tard and C. J. Pickett, *Chem. Rev.*, 2009, **109**, 2245–2274.
- 4 C. Tard, X. M. Liu, S. K. Ibrahim, M. Bruschi, L. De Gioia, S. C. Davies, X. Yang, L. S. Wang, G. Sawers and C. J. Pickett, *Nature*, 2005, **433**, 610–613.
- 5 R. Mejia-Rodriguez, D. S. Chong, J. H. Reibenspies, M. P. Soriaga and M. Y. Darensbourg, *J. Am. Chem. Soc.*, 2004, **126**, 12004–12014.
- 6 G. A. N. Felton, A. K. Vannucci, J. Z. Chen, L. T. Lockett, N. Okumura, B. J. Petro, U. I. Zakai, D. H. Evans, R. S. Glass and D. L. Lichtenberger, *J. Am. Chem. Soc.*, 2007, **129**, 12521–12530.
- 7 L. C. Sun, B. Akermark and S. Ott, *Coord. Chem. Rev.*, 2005, **249**, 1653–1663.
- 8 F. Gloaguen and T. B. Rauchfuss, *Chem. Soc. Rev.*, 2009, **38**, 100–108.
- 9 X. M. Liu, S. K. Ibrahim, C. Tard and C. J. Pickett, *Coord. Chem. Rev.*, 2005, **249**, 1641–1652.
- 10 D. J. Evans and C. J. Pickett, *Chem. Soc. Rev.*, 2003, **32**, 268–275.
- 11 I. P. Georgakaki, L. M. Thomson, E. J. Lyon, M. B. Hall and M. Y. Darensbourg, *Coord. Chem. Rev.*, 2005, **249**, 1133–1133.
- 12 L. C. Song, *Acc. Chem. Res.*, 2005, **38**, 21–28.
- 13 B. E. Barton, G. Zampella, A. K. Justice, L. De Gioia, T. B. Rauchfuss and S. R. Wilson, *Dalton Trans.*, 2010, **39**, 3011–3019.
- 14 D. Morvan, J. F. Capon, F. Gloaguen, A. Le Goff, M. Marchivie, F. Michaud, P. Schollhammer, J. Talarmin, J. J. Yaouanc, R. Pichon and N. Kervarec, *Organometallics*, 2007, **26**, 2042–2052.
- 15 V. Vijaikanth, J. F. Capon, F. Gloaguen, P. Schollhammer and J. Talarmin, *Electrochem. Commun.*, 2005, **7**, 427–430.
- 16 A. L. Goff, V. Artero, R. Metaye, F. Moggia, B. Jousset, M. Razavet, P. D. Tran, S. Palacin and M. Fontecave, *Int. J. Hydrogen Energy*, 2010, DOI: 10.1016/j.ijhydene.
- 17 S. K. Ibrahim, X. M. Liu, C. Tard and C. J. Pickett, *Chem. Commun.*, 2007, 1535–1537.
- 18 K. N. Green, J. L. Hess, C. M. Thomas and M. Y. Darensbourg, *Dalton Trans.*, 2009, 4344–4350.
- 19 X. Ru, X. Zeng, Z. Li, D. J. Evans, C. Zhan, Y. Tang, L. Wang and X. Liu, *J. Polym. Sci., Part A: Polym. Chem.*, 2010, **48**, 2410–2417.
- 20 M. Meldal and C. W. Tornoe, *Chem. Rev.*, 2008, **108**, 2952–3015.
- 21 Z. M. Li, X. H. Zeng, Z. G. Niu and X. M. Liu, *Electrochim. Acta*, 2009, **54**, 3638–3644.
- 22 G. M. Sheldrick, *Acta Crystallogr., Sect. A: Found. Crystallogr.*, 2008, **64**, 112–122.
- 23 F. Gloaguen, J. D. Lawrence, M. Schmidt, S. R. Wilson and T. B. Rauchfuss, *J. Am. Chem. Soc.*, 2001, **123**, 12518–12527.
- 24 F. F. Xu, C. Tard, X. F. Wang, S. K. Ibrahim, D. L. Hughes, W. Zhong, X. R. Zeng, Q. Y. Luo, X. M. Liu and C. J. Pickett, *Chem. Commun.*, 2008, 606–608.
- 25 M. Razavet, S. C. Davies, D. L. Hughes, J. E. Barclay, D. J. Evans, S. A. Fairhurst, X. M. Liu and C. J. Pickett, *Dalton Trans.*, 2003, 586–595.
- 26 Z. Y. Xiao, F. F. Xu, L. Long, Y. Q. Liu, G. Zampella, L. De Gioia, X. R. Zeng, Q. Y. Luo and X. M. Liu, *J. Organomet. Chem.*, 2010, **695**, 721–729.
- 27 J. F. Capon, S. El Hassnaoui, F. Gloaguen, P. Schollhammer and J. Talarmin, *Organometallics*, 2005, **24**, 2020–2022.
- 28 L. L. Duan, M. Wang, P. Li, Y. Na, N. Wang and L. C. Sun, *Dalton Trans.*, 2007, 1277–1283.
- 29 L. C. Song, W. Gao, C. P. Feng, D. F. Wang and Q. M. Hu, *Organometallics*, 2009, **28**, 6121–6130.
- 30 Y. W. Wang, Z. M. Li, X. H. Zeng, X. F. Wang, C. X. Zhan, Y. Q. Liu, X. R. Zeng, Q. Y. Luo and X. M. Liu, *New J. Chem.*, 2009, **33**, 1780–1789.
- 31 X. H. Zeng, Z. M. Li, Z. Y. Xiao, Y. W. Wang and X. M. Liu, *Electrochem. Commun.*, 2010, **12**, 342–345.

- 32 X. H. Zeng, Z. M. Li and X. M. Liu, *Electrochim. Acta*, 2010, **55**, 2179–2185.
- 33 D. Morvan, J. F. Capon, F. Gloaguen, P. Schollhammer and J. Talarmin, *Eur. J. Inorg. Chem.*, 2007, 5062–5068.
- 34 J. W. Tye, J. Lee, H. W. Wang, R. Mejia-Rodriguez, J. H. Reibenspies, M. B. Hall and M. Y. Darensbourg, *Inorg. Chem.*, 2005, **44**, 5550–5552.
- 35 J. F. Capon, F. Gloaguen, F. Y. Petillon, P. Schollhammer and J. Talarmin, *Coord. Chem. Rev.*, 2009, **253**, 1476–1494.
- 36 J. F. Capon, S. Ezzaher, F. Gloaguen, F. Y. Petillon, P. Schollhammer, J. Talarmin, T. J. Davin, J. E. McGrady and K. W. Muir, *New J. Chem.*, 2007, **31**, 2052–2064.
- 37 S. J. Borg, T. Behrsing, S. P. Best, M. Razavet, X. M. Liu and C. J. Pickett, *J. Am. Chem. Soc.*, 2004, **126**, 16988–16999.
- 38 G. A. N. Felton, B. J. Petro, R. S. Glass, D. L. Lichtenberger and D. H. Evans, *J. Am. Chem. Soc.*, 2009, **131**, 11290–11291.
- 39 S. Ott, M. Kritikos, B. Akermark, L. C. Sun and R. Lomoth, *Angew. Chem., Int. Ed.*, 2004, **43**, 1006–1009.